CAMS UWA Node 8 year (2006 to 2013) Research Highlights

Our studies mainly concerned electron correlations, the structure and dynamics of atoms, molecules, surfaces and thin films and positron and positronium interactions with pores and surfaces. The characterization of the interplay between the Coulomb interaction and spin-orbit coupling, led to the concentration on electron spin angular momentum in single atoms and grew to encompass thin films and momentum space behaviour. During the last several years our positron and positronium interests widened and now have many potential industrial applications. Recent advances are indicated earlier in this 2013 annual report. In this section we report an overview of selected earlier achievements, including some instrumentation.

The achievements would not have been possible without the contributions from many people, shown in Figure 53.

Figure 53: Some of the key people in the UWA Node during 2006–2013.

The spin-polarized electron source and beam transport (see Figure 54) **were fundamental instrumentation for many projects**, such as thin film studies (Figure 55), angle resolved momentum and energy detection (Figure 56), a Mini-Mott detector of electron spin (Figure 57) and electron scattering from atoms (Figure 58).

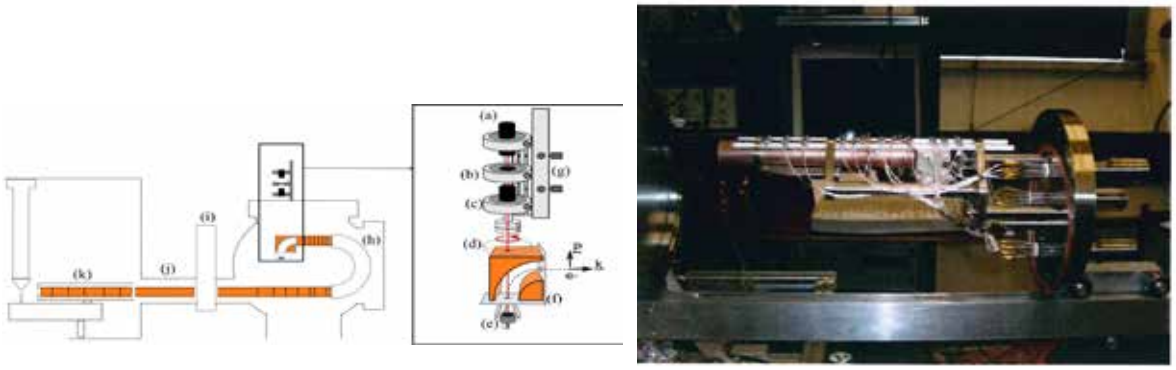

Figure 54: The UWA Polarised electron source. The inset shows the 30mW laser, circular polarizer, photoemission from a GaAs crystal and electron bending through 90˚ to obtain polarization transverse to the momentum vector. Then the polarized beam is energy analysed and transported though a UHV isolation valve into an interaction chamber (upper left). Construction method of the electron transport optics (on right) is also shown.

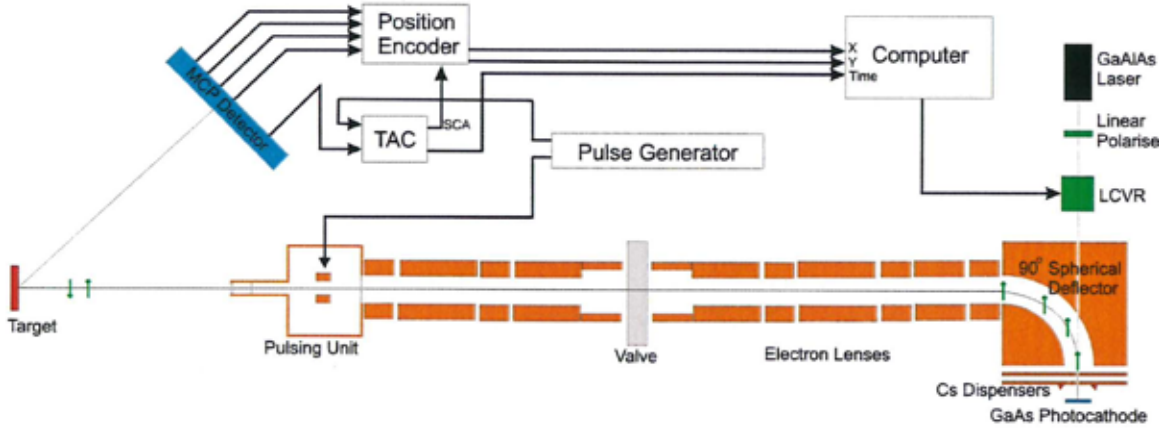

Figure 55: Polarised electron source and beam transport, 20 MHz electron pulser, thin film surface target, and scattered electron detector with a 75 mm channel plate incorporating position encoder, nanosec timing and recording.

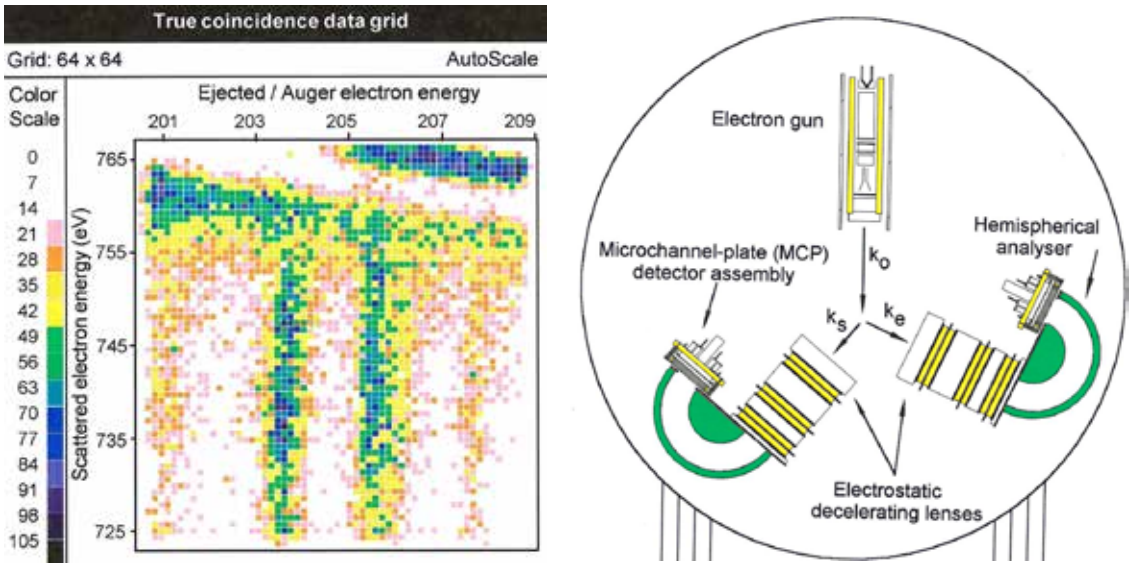

Figure 56: Electron pair, angle resolved momentum and energy detection. Right figure represents a typical scattering instrument. Left figure indicates an electron coincidence pair of Auger and ejected electrons from Argon.

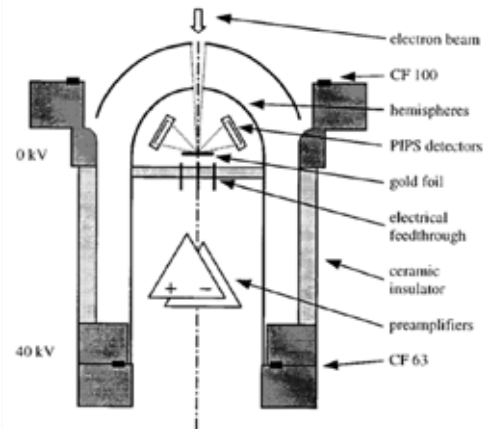

Figure 57: The Mini-Mott detector of electron spin [24] has been operating on the incident polarized electron pair measurements, on thin films, and on our JEOL SEM for surface analysis.

Figure 58: Picture showing the electron scattering from atoms apparatus.

Electron correlations in the inert gas atoms were reported in over 20 papers. They contain an extensive description of photon excitation functions, emission and energy loss functions, cross sections for excitation of many states; photon polarizations, spin-dependent measurements with high resolution 50–120 meV electron beams, and spin polarizations of 28% and 75%; spin up-down asymmetries and Stokes parameters.

Electron impact excitation of neon atoms. Typical achievements are indicated for the 8 detected wavelengths of neon atoms shown in Figure 59.

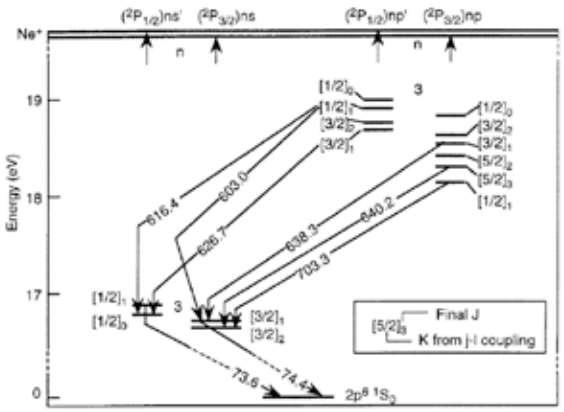

Figure 59: Eight detected wavelengths of neon atoms in our studies.

1) Transitions from a common upper state, with $\Delta J = 1$, had larger linear polarizations than those with $\Delta J = 0$ and -1.

2) Transitions from upper states with a different core state, those with a $^2P_{1/2}$ core had a larger linear polarization than those with a $^2P_{3/2}$ core.

Results 1) and 2) indicated the role of angular momentum coupling in electronic excitation.

3) The multipole moment, Im T(J)11, reflects electron exchange, while the Re T(J)21 indicates the strength of spin–orbit interaction within the atom. They are consistent with the calculated LS compositions.

4) Breakdown of LS-coupling for J = 1 states in the neon 3p manifold were confirmed. Spin–orbit interaction within the atom plays a significant role in the excitation.

Results 3) and 4) indicate correlated wave functions and mixing coefficients.

5) The negative ion resonances had a significant influence on the polarizations, which depended on the LS mixing properties of the intermediately coupled states.

6) The effect of the core on the alignment of the excited states indicates resonances have more influence on alignment of excited states with a j = 1/2 core than for a j = 3/2 core.

Results 5) and 6) indicate the angular momentum coupling in the excitation process, the importance of observing the polarization of the transition radiation as well as the need for modeling and for angular correlation measurements.

Excitation of zinc atoms to singly, doubly and triply excited states and the $3d^9\,4s^2\,4p$ autoionizing states. These studies observed the dipole decay photons from the singly excited 4d, 5d and 6d states (see Figure 60), from direct excitation, for a wide range on incident energies and for cascade decay from doubly and triply excited states of the neutral atom. Collision processes revealed considerable auto-ionizing and negative ion formation indicating the effect on the inner d-shell electrons.

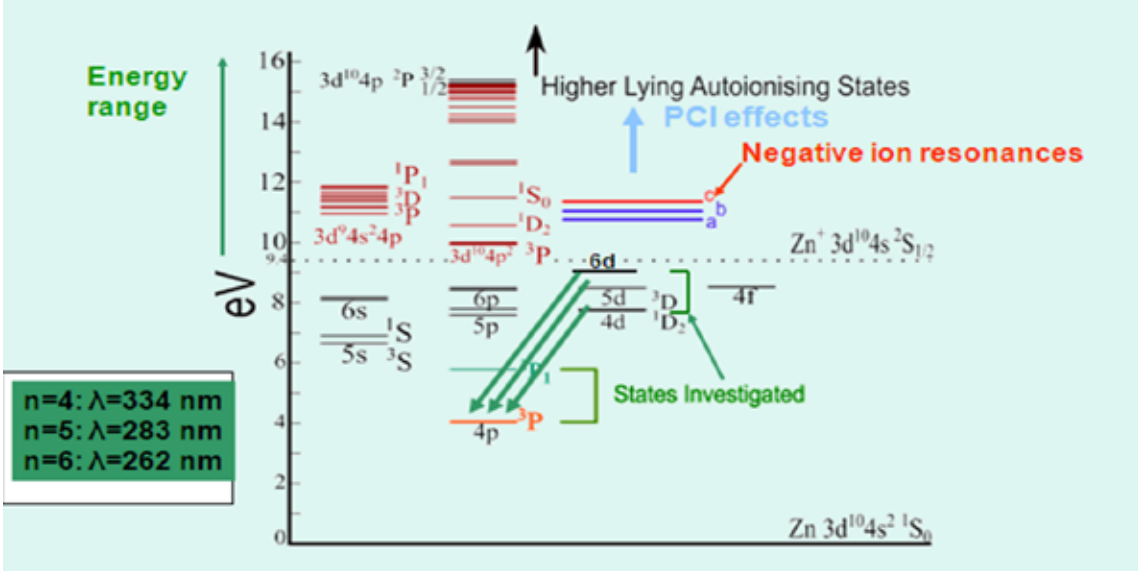

Figure 60: Excitation of zinc to singly, doubly and triply excited states and the $3d^9 4s^2 4p$ autoionizing states.

Figures 61 and 62 indicate many of the significant features of the scattering processes.

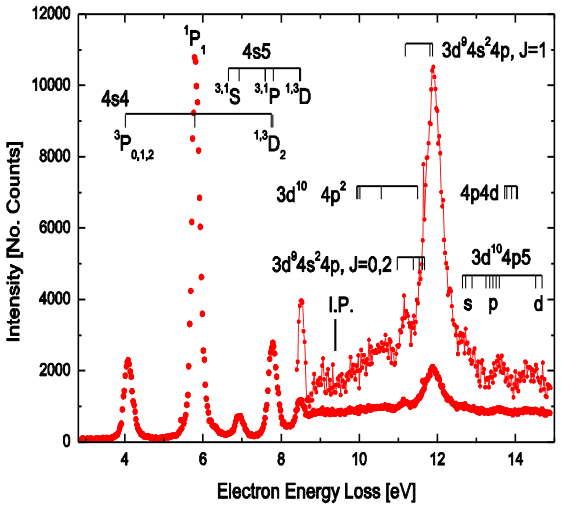

Figure 61: Typical electron energy loss features of zinc atoms from 4 to 14 eV, with known excited states below the ionization threshold with strong excitation of the nd $^3D_{1,2,3}$ states for n=4, 5 and 6.

The features in Figure 62 indicate highly correlated electronic configurations, initial, intermediate and final state configuration interactions (valence–core, core–core, valence–valence), breakdown of LS coupling, spin-orbit, exchange, short lived negative ion resonances, all in the post collision interaction processes which continues as an active research field. This knowledge has universal applicability as a continuing scientific basis for research, education and industries. It provides cutting-edge research to keep Australia at the international forefront of atomic interactions. The investigations promote our understanding of physical and chemical properties of atoms, molecules and materials. The significance of this breakthrough science rests on these interatomic interactions originating from the distribution of electronic charge and spin which determine properties and functions of complex compounds.

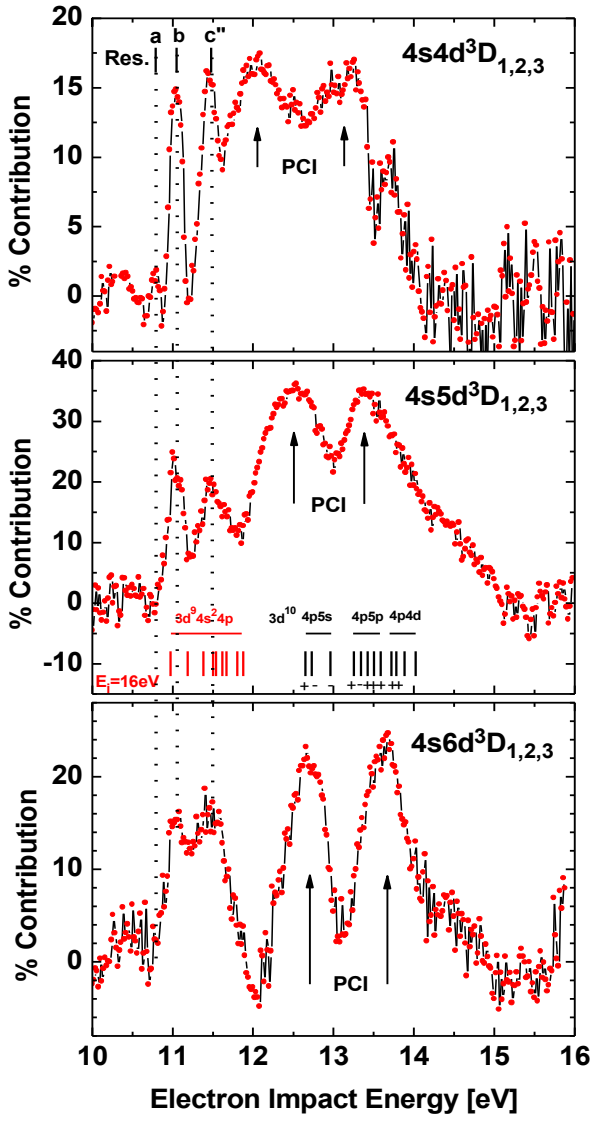

Figure 62: Post Collision Interaction (PCI) effects in zinc atoms just above the ionization threshold, as observed in each of the emitted 3d, 4d and 5d dipole photons.

Positron Annihilation Lifetime Spectroscopy (PALS) and Coincidence Doppler Spectroscopy (CDB) were used to study vacancies and porosities of various materials with industrial uses.

Geopolymers are a class of inorganic polymers that are based on aluminosilicates:

- They are a potential replacement for traditional building materials such as ordinary Portland cements.
- Advantages: superior fire and acid resistance, and their manufacture requires a much lower calcining temperature, producing only 20% of the CO_2 per unit mass compared to ordinary cement.
- The microstructure and resultant properties of these materials depend predominantly on the M_2O: SiO_2:Al_2O_3: H_2O molar ratios, where M = Li^+, Na^+, K^+, Rb^+ or Cs^+.

Semiconductors—vacancies/defects can be used to control electronic and optical properties.

Metals or Alloys—formation of vacancies and voids can lead to embrittlement and failure.

Pores in materials—increased surface area and provide sites for the storage of molecules.

Polymers—pores of different sizes can be used to encapsulate, release and separate molecules.

Pyrochlore materials of the form $A_2B_2O_7$ where A is a transition metal La or rare-earth element such as Y, Pr, Eu, and B is Re, Ir, Os or Ir are studied because of the extensive compositional range of the compounds which exhibit a variety of applications, e.g. dielectric materials, catalysts, solid electrolytes, thermal barrier coatings, new topological phases and actinide host phases for nuclear waste encapsulation.

Cementitious materials—The mechanical properties of cementitious materials are heavily influenced by porosity, since the volume and size distribution of pores control both their strength and durability.

Low energy positron interaction with surfaces

Interaction of low energy positrons with a W(001) surface, as well as with an oxidized W surface, and thin films of Fe, Ni, LiF, Ag and Au deposited on W(001) were studied. Positron work functions, re-emission of positrons and their angular and energy distribution from these surfaces were investigated. An attempt was also made to study a positron energy structure of W(001), by measuring the reflectivity of very low energy positrons from the surface.

References

[1] E. R. Vance, J. H. Hadley, Jr. and F. H. Hsu, *J. Aust. Ceram. Soc.* **44**[1], 53–6 (2008).

[2] I. Bray and A. T. Stelbovics, *Phys. Rev. A* **46**, 6995–7011 (1992).

[3] M. C. Zammit, D. V. Fursa and I. Bray, *Phys. Rev. A* **87**, 020701 (2013).

[4] I. B. Abdurakhmanov, A. S. Kadyrov, D. V. Fursa and I. Bray, *Phys. Rev. Lett.* **111**, 173201 (2013).

[5] A. S. Kadyrov, A. V. Lugovskoy, R. Utamuratov and I. Bray, *Phys. Rev. A* **87**, 060701 (2013).

[6] M. C. Zammit, D. V. Fursa and I. Bray, *Phys. Rev. A* **88**, 062709 (2013).

[7] J. D. Builth-Williams, S. M. Bellm, L. Chiari, P. A. Thorn, H. Chaluvadi, D. H. Madison, C. G. Ning, B. Lohmann, G. B. da Silva and M. J. Brunger, *J. Chem. Phys.* **139**, 034306 (2013).

[8] P. Drossart, B. Bézard, S. Atreya, J. Lacy, E. Serabyn, A. Tokunaga and T. Encrenaz, *Icarus* **66**, 610–8 (1986).

[9] L. Chiari, A. Zecca, G. García, F. Blanco and M. J. Brunger, *Journal of Physics B* **46**, 235202 (2013).

[10] L. Chiari, A. Zecca, E. Trainotti, G. García, F. Blanco, M. H. F. Bettega, S. d'A. Sanchez, M. T. do N. Varella, M. A. P. Lima and M. J. Brunger, *Physical Review A* **88**, 022708 (2013).

[11] L. Chiari, A. Zecca, E. Trainotti, M. H. F. Bettega, S. d'A. Sanchez, M. T. do N. Varella, M. A. P. Lima and M. J. Brunger, *Physical Review A* **87**, 032707 (2013).

[12] M. T. do N. Varella, S. d'A. Sanchez, M. H. F. Bettega, M. A. P. Lima, L. Chiari, A. Zecca, E. Trainotti and M. J. Brunger, *Journal of Physics B* **46**, 175202 (2013).

[13] N. Garland, M. Brunger, G. Garcia, J. de Urquijo and R.D. White, *Phys. Rev. A* **88**, 062712 (2013).

[14] S. Dujko, A. Markosyan, R.D. White and U. Ebert, *J. Phys. D* **46** 475202 (2013).

[15] G. Boyle, M. J. E. Casey, R.D. White and J. Mitroy, *Phys. Rev. A* (accepted).

[16] R. I. Campeanu and J. W. Humberston, *J. Phys. B* **10**, 239 (1977).

[17] R. D. White, W. Tattersall, G. Boyle, R. E. Robson, S. Dujko, Z. Lj. Petrovic, A. Bankovic, M. J. Brunger, J. P. Sullivan, S. J. Buckman and G. Garcia, *Applied Radiation and Isotopes* **83**, 77–85 (2014).

[18] Z. Lj. Petrović, S. Marjanović, S. Dujko, A. Banković, G. Malović, S. J. Buckman, G. Garcia, R. D. White and M. J. Brunger, *Applied Radiation and Isotopes* **83**, 148–154 (2014).

[19] A. Armin, G. Juska, B. W. Philippa, P. L. Burn, P. Meredith, R. D. White and A. Pivrikas, *Adv. Energy Mat.* **3**, 321–327 (2013).

[20] C. Vijila, S. P. Singh, E. Williams, P. Sonar, A. Pivrikas, B. Philippa, R. D. White, E. N. Kumar, S. G. Sandhya, S. Gorelik, J. Hobley, A. Furube, H. Matsuzaki and R. Katoh, *J. Appl. Phys.* **114**, 184503 (2013).

[21] S. A. Komolov and L. T. Chadderton, *Surface Science* **90**, 359–380 (1979).

[22] V. N. Strocov and H. I. Starnberg, *Phys. Rev B* **52**, 8759 (1995).

[23] J. A. Baker, M. Touat and P. G. Coleman, *J. Phys. C: Solid State Phys.* **21**, 4713 (1988).

[24] V. N. Petrov, V. V. Grebenshikov, B. D. Grachev and A. S. Kamochkin, *Rev. Sci. Instrum.* **74**,1278 (2003).